Bioorganic Chemistry 58 (2015) 88–95

Contents lists available at ScienceDirect

Bioorganic Chemistry

journal homepage: www.elsevier.com/locate/bioorg

# Spectroscopic investigation of the interaction of water-soluble azocalix[4]arenes with bovine serum albumin

Ping Fan [a,*], Lu Wan [a], Yunshan Shang [b], Jun Wang [a], Yulong Liu [a], Xiaoyu Sun [a], Chen Chen [a]

[a] College of Chemistry, Liaoning University, Shenyang 110036, PR China
[b] State Key Laboratory of Heavy Oil Processing, The Key Laboratory of Catalysis of CNPC, China University of Petroleum, Changping, Beijing 102249, PR China

ARTICLE INFO

*Article history:*
Received 3 July 2014
Available online 16 December 2014

*Keywords:*
Interaction
Azocalix[4]arene derivatives
Bovine serum albumin (BSA)
Fluorescence spectroscopy

ABSTRACT

In this work, three hydrosoluble azocalix[4]arene derivatives, 5-(*o*-methylphenylazo)-25,26,27-tris(carboxymethoxy)-28-hydroxycalix[4]arene (*o*-MAC-Calix), 5-(*m*-methylphenylazo)-25,26,27-tris(carboxymethoxy)-28-hydroxycalix[4]arene (*m*-MAC-Calix) and 5-(*p*-methylphenylazo)-25,26,27-tris(carboxy methoxy)-28-hydroxycalix[4]arene (*p*-MAC-Calix) were synthesized. Their structures were characterized by infrared spectrum (IR), nuclear magnetic resonance spectrum ($^1$H NMR and $^{13}$C NMR) and mass spectrum (MS). The interactions between these compounds and bovine serum albumin (BSA) were studied by fluorescence spectroscopy, UV–vis spectrophotometry and circular dichroic spectroscopy. According to experimental results, three azocalix[4]arene derivatives can efficiently bind to BSA molecules and the *o*-MAC-Calix displays more efficient interactions with BSA molecules than *m*-MAC-Calix and *p*-MAC-Calix. Molecular docking showed that the *o*-MAC-Calix was embedded in the hydrophobic cavity of helical structure of BSA molecular and the tryptophan (Trp) residue of BSA molecular had strong interaction with *o*-MAC-Calix. The fluorescence quenching of BSA caused by azocalix[4]arene derivatives is attributed to the static quenching process. In addition, the synchronous fluorescence spectroscopy indicates that these azocalix[4]arene derivatives are more accessible to Trp residues of BSA molecules than the tyrosine (Tyr) residues. The circular dichroic spectroscopy further verified the binding of azocalix[4]arene derivatives and BSA.



## 1. Introduction

Calixarene is made up of phenol linked via methylene groups, which can exhibit weak fluorescence. Calixarene is a flexible molecular scaffold for its unique cavity structure, excellent ion sensing properties, and easy modifications [1–5]. In many cases, the azo moiety is introduced into the upper rim of calixarenes to monitor the binding process upon complexation with ions and molecules. Many studies on azocalixarene derivatives also involved the functionalization of the lower rim with chelating groups, such as carboxylic acid, ester and other groups. As a result, the modified azocalix[4]arene derivatives can form chromogenic sensor and fluorescent sensor [6–11]. Recently, the triazole linked anthracenyl appended calix[4]arene that used for recognition of Co(II) had been reported by Rao and co-workers [12]. They had also designed and synthesized the 1,3-di-amidoquinoline conjugate of calix[4]arene as a ratiometric and colorimetric sensor for Zn(II) [13].

In recent years, several reported water-solution calix[4]arene derivatives, had showed lots of applications in biological aspects, such as drug delivery, inhibitor of infection, antibacterial agents, identification and detection of the organisms protein [14–21]. However, the azocalix[4]arene derivatives were few used in biology. Some biological studies related to plasmid DNA binding were reported by Ungaro and co-workers [22–24]. A series of calix[4]arene derivatives with modified guanidinium groups in the upper and lower rims were synthesized. These calix[4]arenes were used to investigate DNA condensation, toxicity and cell transfection properties, etc. [22,23]. Some of hydrophilic derivatives had also showed interesting levels of bioactivity against bacteria, fungi, cancerous cells, and enveloped viruses [24].

As we all known, the protein is a kind of important biological macromolecules, which is the most abundant in the function material of biological systems. Compared with other biological molecules, the serum albumins (SA) are the most sufficient proteins in the plasma, and also show many physiological functions [25–27]. What is more, the structure of BSA molecule is similar to human serum albumins (HSA) molecule in 76%, therefore, BSA molecules are used as the study model [28,29]. Koh and his coworkers used

* Corresponding author. Fax: +86 024 62202053.
*E-mail address:* pingfan_bft@126.com (P. Fan).

http://dx.doi.org/10.1016/j.bioorg.2014.12.002
0045-2068/

self-assembled calix[4]arene carboxylic acid derivative monolayers for protein immobilization with BSA as a model. Shahgaldian and co-workers synthesized three amphiphilic dodecanoyl calix[4]arene derivatives and investigated the interactions of their solid lipid nanoparticles with BSA [30,31]. It is expected that calix[4]arene derivatives should have a variety of potential functions in biological research.

For exploring further systematic applications of calix[4]arene derivatives in biological systems, three novel calix[4]arene derivatives, containing the hydrophilic groups-carboxyl groups to interact with biological protein and the azobenzene moiety for a better visual observant were synthesized. In this research, BSA was used as a model protein. The maximum value of intrinsic fluorescence and synchronous fluorescence spectrum were used to determine the interaction pattern and the binding sites of the azocalix[4]arene derivatives to BSA molecules, respectively. This research supplied original reference of hydrosoluble azocalix[4]arene derivatives interact with protein molecules.

## 2. Experimental section

### 2.1. Reagents

Commercially prepared bovine serum albumin (BSA, purity >99.0%) was purchased from Beijing Abxing Biological Technology Company and stored in refrigerator at 4.0 °C. The Tris (hydroxylmethyl) aminomethane (Tris), HCl and NaCl were all of analytical reagent grade, and double distilled water was used for all solution preparation. The solvents for synthesis of azocalix[4]arene derivatives were purchased from Bodi (Tianjin, China) and were treated with molecular sieves to remove water before use.

### 2.2. Apparatus

The IR spectra were determined by Fourier transform infrared spectrophotometer (Spectrum 100, Perkin-Elmer Company, USA). The $^1$H NMR and $^{13}$C NMR spectra were recorded with nuclear magnetic double resonance spectrometer (Mercury 300, Varian Company, USA). The mass spectra were measured on the OTOF-Q Micromass instrument (Bruker Varian, Germany) and LC–MSD-Trap/SL (Agilent 1100 Varian Company, USA) using electrospray ionization methods. The fluorescence measurements were performed with fluorophotometer (Cary 300, Varian Company, USA) and the UV–vis absorption spectra were recorded with UV–vis spectrophotometer (Cary 50, Varian Company, USA). Circular dichroism (CD) measurements were performed by a J-810 spectro polarimeter (JASCO, Japan) using a 1.0 cm quartz cell.

### 2.3. Syntheses of calixarene derivatives

Compounds **1–3** were synthesized according to previously described methods [32,33]. The synthesis of the other compounds **4**, **5a**, **5b**, **5c**, **6a** (*o*-MAC-Calix), **6b** (*m*-MAC-Calix) and **6c** (*p*-MAC-Calix) were first reported in this study (Scheme 1).

Under a nitrogen stream, calix[4]arene **3** and ethyl bromoacetate in a 1:1.5 M ratio were added to dry acetonitrile using $CaH_2$ as catalyst, the mixture was refluxed for 24 h. The suspension was allowed to cool at room temperature. Then the inorganic salts were removed by filtration and the volatiles were removed under reduced pressure to give an oil mixture. The oil was washed with dichloromethane and concentrated to dryness. The compound **4** was obtained after recrystallization. The compounds **5a**, **5b** and **5c** were also synthesized according to previously described methods [34].

*o*-MAC-Calix, *m*-MAC-Calix and *p*-MAC-Calix were synthesized in a similar manner to that reported in a previous paper with raw materials of compound **5a**, **5b** and **5c**, yield 94%, 95% and 95% as yellow solids [35]. Spectroscopy data are as follows respectively.

*o-MAC-Calix:* Mp 257–260 °C. ESI–MS (*m*/*z*): 739.22 (M + Na); 717.24 (M + H). IR (KBr pellet, $cm^{-1}$): 3394, 2926, 1721, 1343. $^1$H NMR (300 MHz, DMSO-$d_6$), δ (ppm): δ 7.73 (s, 2H), 7.48 (d, *J* = 8.0 Hz, 1H), 7.38 (d, *J* = 6.3 Hz, 2H), 7.32–7.26 (m, 1H), 7.18 (d, *J* = 7.6 Hz, 2H), 6.85 (q, *J* = 6.1 Hz, 5H), 6.66 (t, *J* = 7.5 Hz, 2H), 4.83 (s, 2H), 4.75 (d, *J* = 11.2 Hz, 4H), 4.47 (d, *J* = 14.6 Hz, 4H), 3.36 (d, *J* = 13.0 Hz, 4H), 2.66 (s, 3H). $^{13}$C NMR (75 MHz, DMSO-$d_6$) δ 171.08, 170.73, 156.28, 154.66, 154.02, 150.37, 145.40, 136.72, 135.30, 133.98, 132.61, 131.34, 130.29, 129.40, 129.33, 129.00, 128.86, 128.71, 126.61, 124.43, 123.79, 115.17, 72.12, 70.76, 30.92, 30.56, 17.30.

*m-MAC-Calix:* Mp 269–273 °C decompose. ESI–MS (*m*/*z*): 715.0 (M–H), 752.9 (M–H + K). IR (KBr pellet, $cm^{-1}$): 3390, 2925, 1724, 1343. $^1$H NMR (300 MHz, DMSO-$d_6$) δ 7.75 (s, 2H), 7.63 (d, *J* = 6.3 Hz, 2H), 7.44 (t, *J* = 8.0 Hz, 1H), 7.31 (d, *J* = 7.5 Hz, 1H), 7.19 (d, *J* = 7.5 Hz, 2H), 6.92–6.80 (m, 5H), 6.71–6.63 (m, 2H), 4.87–4.68 (m, 6H), 4.56–4.40 (m, 4H), 3.55 (d, *J* = 12.8 Hz, 2H), 3.36 (d, *J* = 9.9 Hz, 2H), 2.39 (s, 3H). $^{13}$C NMR (75 MHz, DMSO-$d_6$) δ 171.15, 170.84, 156.48, 154.70, 154.08, 152.51, 145.00, 138.94, 135.38, 134.08, 132.67, 131.19, 129.44, 129.31, 129.11, 128.97, 128.86, 124.60, 124.10, 123.83, 119.97, 72.22, 70.91, 31.03, 30.72, 21.16.

*p-MAC-Calix:* Mp 255–257 °C. ESI–MS (*m*/*z*): 739.22 (M + Na); 717.24 (M + H). IR (KBr pellet, $cm^{-1}$): 3392, 2926, 1714, 1343. $^1$H NMR (300 MHz, DMSO-$d_6$) δ 7.78–7.67 (m, 4H), 7.35 (d, *J* = 8.3 Hz, 2H), 7.17 (d, *J* = 7.6 Hz, 2H), 6.87 (d, *J* = 7.3 Hz, 5H), 6.66 (t, *J* = 7.5 Hz, 2H), 4.82 (s, 2H), 4.74 (d, *J* = 9.7 Hz, 4H), 4.54–4.40 (m, 4H), 3.36 (d, *J* = 12.9 Hz, 4H), 2.38 (s, 3H). $^{13}$C NMR (75 MHz, DMSO-$d_6$) δ 171.09, 170.81, 156.26, 154.65, 154.06, 150.44, 144.88, 140.50, 135.32, 134.04, 132.67, 130.13, 129.49, 129.37, 129.04, 128.91, 128.80, 124.51, 124.08, 123.64, 122.21, 72.21, 70.85, 40.15, 30.95, 30.65, 21.11.

### 2.4. Measurement of binding parameters

The binding parameters of BSA and three azocalix[4]arene derivatives (*o*-MAC-Calix, *m*-MAC-Calix and *p*-MAC-Calix) were measured by fluorescence spectroscopy method. BSA solution was prepared in 0.05 mol/L Tris–HCl–NaCl buffer solution (pH = 7.40 and containing 0.05 mol/L NaCl) for keeping the solution acidity and ionic strength. The concentration was $2.00 \times 10^{-5}$ mol/L. Azocalix[4]arene derivatives were prepared in 0.05 mol/L Tris–HCl–NaCl buffer solution and its concentration was $5.00 \times 10^{-5}$ mol/L. The 12.50 mL BSA stock solution and the appropriate volume of azocalix[4]arene derivatives stock solution were added into a 25.00 mL volumetric flask and diluted with Tris–HCl–NaCl buffer solution. The final BSA concentration was $1.00 \times 10^{-5}$ mol/L, and the concentration of azocalix[4]arene derivatives vary from $0.00 \times 10^{-5}$ mol/L to $2.50 \times 10^{-5}$ mol/L at an increment of $0.50 \times 10^{-5}$ mol/L. The fluorescence spectra of BSA solutions along with the increase of azocalix[4]arene derivatives were recorded in the wavelength of 250–500 nm upon excitation wavelength at 278 nm using a slit width of 5.0 nm. The tested solutions were incubated for 10 min before the measurement and the curves of fluorescence spectrum were got at 37.00 ± 0.02 °C. For the calculation of quenching parameters, the maximal intensities of BSA intrinsic fluorescence were recorded at 345 nm. According to the fluorescent data, the calculated quenching rate constants, apparent binding association constants, average numbers of binding sites and the binding distances were showed in Fig. 1. The corresponding parameters were offered in Table 1.

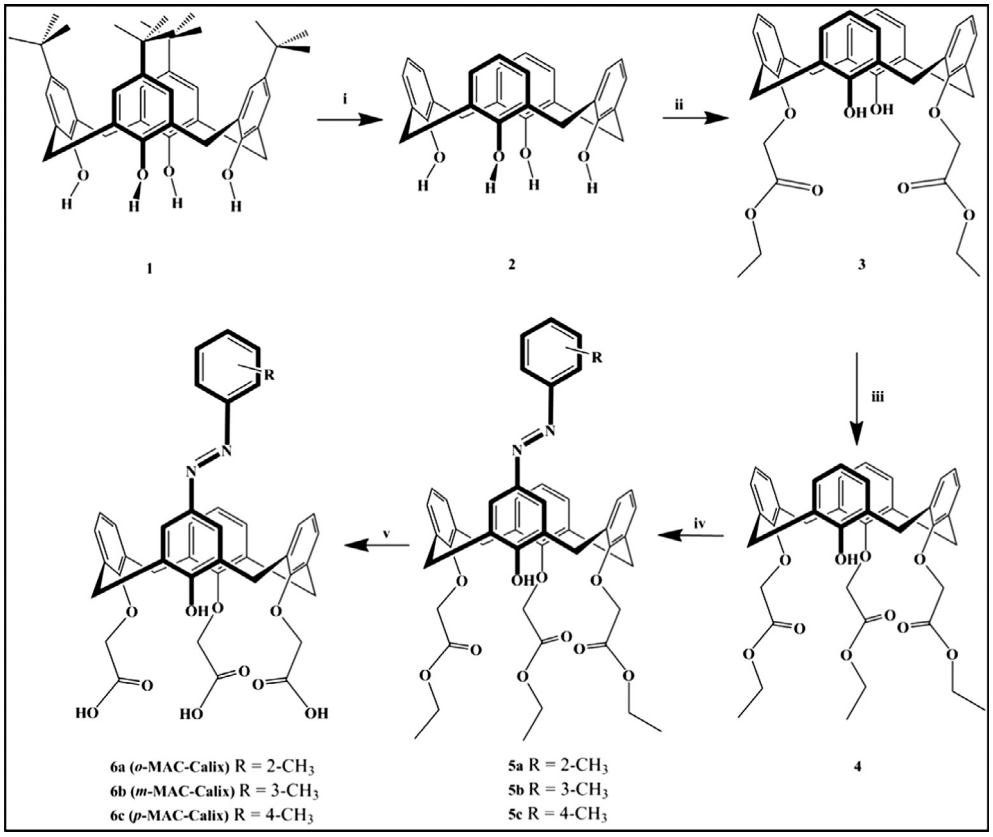


**Scheme 1.** Synthesis of compounds **4**, **5a**, **5b**, **5c**, **6a** (*o*-MAC-Calix), **6b** (*m*-MAC-Calix) and **6c** (*p*-MAC-Calix). Reagents and conditions: (i) toluene, aluminum trichloride, rt, 3 h; (ii) $K_2CO_3$, $BrCH_2COOEt$, $CH_3CN(S)$ , refluxed 16 h; (iii) $CaH_2$ , $BrCH_2COOEt$, dry$CH_3CN(S)$, refluxed 24 h; (iv) (2) aromatic amine/acetone, $NaNO_2$/4 N HCl, pyridine, 0 °C, 5 h; (v) 15%NaOH, THF, $CH_3CH_2OH$, refluxed 24 h.

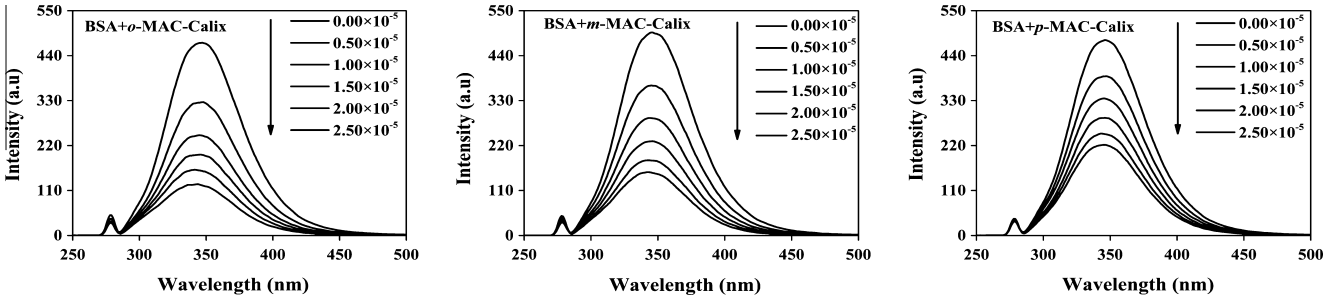


**Fig. 1.** Fluorescence spectra of BSA + *o*-MAC-Calix, BSA + *m*-MAC-Calix and BSA + *p*-MAC-Calix solutions with *o*-MAC-Calix, *m*-MAC-Calix and *p*-MAC-Calix concentrations (from $0.00 \times 10^{-5}$ mol/L to $2.50 \times 10^{-5}$ mol/L at $0.50 \times 10^{-5}$ mol/L intervals) ([BSA] = $1.00 \times 10^{-5}$ mol/L, [Tris–HCl] = [NaCl] = 50 mmol/L, pH = 7.40, $T_{solu}$ = 37.00 ± 0.02 °C and $V_{total}$ = 25.00 mL).

In controlled experiment, four 12.5 mL BSA stock solutions were added to four 25.0 mL volumetric flasks marked as a–d. And then, 5.0 mL three azocalix[4]arene derivatives stock solutions were added into above volumetric flasks b, c and d, respectively. Finally, all of the solutions were diluted to the mark with Tris–HCl–NaCl buffer solution. The final BSA and azocalix[4]arene derivatives concentration were both $1.00 \times 10^{-5}$ mol/L. Each of the sample solutions was also measured by Circular dichroism (CD) spectrometer.

## 3. Results and discussion

### 3.1. Fluorescence Spectra of BSA solution with azocalix[4]arene derivatives (o-MAC-Calix, m-MAC-Calix and p-MAC-Calix)

As a protein molecule, bovine serum albumin (BSA) naturally fluoresces around 345 nm (at 278 nm excitation), which is mainly attributed to tryptophan (Trp), tyrosine (Tyr) and phenylalanine (Phe) residues. As could be seen in Fig. 1, the intrinsic fluorescence of BSA molecules at 345 nm could be greatly quenched by azocalix[4]arene derivatives (*o*-MAC-Calix, *m*-MAC-Calix and *p*-MAC-Calix). It is confirmed that this is owing to the effect of the interaction of azocalix[4]arene derivatives as quencher with BSA.

### 3.2. Binding constant and binding site number

The interaction between the azocalix[4]arene derivatives and BSA molecules in Tris–HCl–NaCl buffer solution could be studied by measuring the change of intrinsic fluorescence of BSA molecules around 345 nm in the presence of azocalix[4]arene derivatives with different concentrations. The data of fluorescence intensities could be analyzed by using the Stern–Volmer Eq. (1):

**Table 1**
Quenching constants ($K_{sv}$ and $K_q$), binding constants, stable constants and binding site numbers calculated according to Stern–Volmer plots, Lineweaver–Burk plots and double logarithm plots of BSA + *o*-MAC-Calix, BSA + *m*-MAC-Calix and BSA + *p*-MAC-Calix solutions with *o*-MAC-Calix, *m*-MAC-Calix and *p*-MAC-Calix concentrations. (from $0.00 \times 10^{-5}$ mol/L to $2.50 \times 10^{-5}$ mol/L at $0.50 \times 10^{-5}$ mol/L intervals) ([BSA] = $1.00 \times 10^{-5}$ mol/L, [Tris–HCl] = [NaCl] = 50 mmol/L, pH = 7.40, $T_{solu}$ = 37.00 ± 0.02 °C and $V_{total}$ = 25.00 mL).

| System | Stern–Volmer plot | $R^2$ | $K_{sv}$ (L/mol) | $K_q$ (L/mol·s) |
|---|---|---|---|---|
| *o*-MAC-Calix | $F_0/F = 1.0178[Q] + 1$ | 0.9826 | $1.0178 \times 10^5$ | $1.0178 \times 10^{13}$ |
| *m*-MAC-Calix | $F_0/F = 0.8409[Q] + 1$ | 0.9885 | $8.4090 \times 10^4$ | $8.4090 \times 10^{12}$ |
| *p*-MAC-Calix | $F_0/F = 0.4571[Q] + 1$ | 0.9980 | $4.5710 \times 10^4$ | $4.5710 \times 10^{12}$ |

| System | Lineweaver–Burk plot | $R^2$ | $f$ | $K_{LB}$ (L/mol) | $K_D$ (mol/L) |
|---|---|---|---|---|---|
| *o*-MAC-Calix | $1/[(F_0 - F)/F_0] = 1.1598/[Q] + 0.925$ | 0.9994 | 1.0811 | $7.9755 \times 10^4$ | $1.2538 \times 10^{-5}$ |
| *m*-MAC-Calix | $1/[(F_0 - F)/F_0] = 1.4878/[Q] + 0.8615$ | 0.9997 | 1.1608 | $5.7904 \times 10^4$ | $1.7270 \times 10^{-5}$ |
| *p*-MAC-Calix | $1/[(F_0 - F)/F_0] = 2.2052/[Q] + 1.0210$ | 0.9976 | 0.9794 | $4.6300 \times 10^4$ | $2.1598 \times 10^{-5}$ |

| System | Double logarithm plot | $R^2$ | $K_A$ (L/mol) | $n$ | $\Delta G^0$(kJ/mol) |
|---|---|---|---|---|---|
| *o*-MAC-Calix | $\log[(F_0 - F)/F] = 1.1048\log[Q] + 5.4939$ | 0.9949 | $3.118 \times 10^5$ | 1.1048 | −32.604 |
| *m*-MAC-Calix | $\log[(F_0 - F)/F] = 1.1414\log[Q] + 5.5858$ | 0.9977 | $3.853 \times 10^5$ | 1.1414 | −33.149 |
| *p*-MAC-Calix | $\log[(F_0 - F)/F] = 1.0194\log[Q] + 4.7480$ | 0.9973 | $5.598 \times 10^4$ | 1.0194 | −28.177 |

$$F_0/F = 1 + K_{SV}[Q_F] = 1 + K_q\tau_0[Q_F] \quad (1)$$

where the $F_0$ and $F$ are the fluorescence intensities of BSA solutions at 345 nm in the absence and presence of azocalix[4]arene derivatives with various concentrations, respectively. $K_q$ is the apparent quenching constant of bimolecular fluorescence, $\tau_0$ is the life time of the fluorophore, $K_{sv}$ is the Stern–Volmer fluorescence quenching constant and $[Q_F]$ is the concentration of azocalix[4]arene derivatives as a quencher.

Fig. 2a displayed the Stern–Volmer plots of BSA solutions in the presence of azocalix[4]arene derivatives with various concentrations. All three plots exhibited a comparatively good linear relationship ($R^2$ = 0.9826 for BSA + *o*-MAC-Calix system, $R^2$ = 0.9885 for BSA + *m*-MAC-Calix system and $R^2$ = 0.998 for BSA + *p*-MAC-Calix system). From Stern–Volmer Eq. (1), the $K_{sv}$ of these three systems could be obtained ($K_{sv} = 1.0178 \times 10^5$ L/mol for BSA + *o*-MAC-Calix system, $K_{sv} = 8.4090 \times 10^4$ L/mol for BSA + *m*-MAC-Calix system and $K_{sv} = 4.5710 \times 10^4$ L/mol for BSA + *p*-MAC-Calix system). In general, for the most of protein molecules, the $\tau_0$ is known to be approximately $10^{-8}$ s. Therefore, the $K_q$ could be calculated ($K_q = 1.0178 \times 10^{13}$ L/mol·s for BSA + *o*-MAC-Calix system, $K_q = 8.4090 \times 10^{12}$ L/mol·s for BSA + *m*-MAC-Calix system and $K_q = 4.5710 \times 10^{12}$ L/mol·s for BSA + *p*-MAC-Calix system) and all corresponding results were showed in Table 1. It can be seen that the array order is $K_{q(BSA+o\text{-MAC-Calix})} > K_{q(BSA+m\text{-MAC-Calix})} > K_{q(BSA+p\text{-MAC-Calix})}$. All of the above $K_q$ values are greater than the maximum value ($2.0 \times 10^{10}$ L/mol s) of the diffusion controlled quenching process of biological macromolecules. The results provide preliminary evidences that the dominating quenching mechanism may be static and the azocalix[4]arene derivatives have interaction with BSA molecules [36].

To further confirm that the fluorescence quenching mechanisms of azocalix[4]arene derivatives to BSA static quenching are process, the fluorescence quenching data was analyzed again according to the Lineweaver–Burk double reciprocal equation (modified Stern–Volmer equation or double reciprocal) (2).

$$1/[(F_0 - F)/F_0] = 1/(fK_{LB}[Q_F]) + 1/f \quad (2)$$

In the present case, $F_0$, $F$ and $Q_F$ are same as Eq. (1). The $f$ is the fraction of accessible fluorescence, and the $K_{LB}$ is the static fluorescence quenching association constant. From the corresponding plots in Fig. 2b and dates in Table 1, the $f$ and $K_{LB}$ could be obtained ($f$ = 1.0811 and $K_{LB} = 7.9755 \times 10^4$ L/mol for BSA + *o*-MAC-Calix system, $f$ = 1.1608 and $K_{LB} = 5.7904 \times 10^4$ L/mol for BSA + *m*-MAC-Calix system and $f$ = 0.9794 and $K_{LB} = 4.6300 \times 10^4$ L/mol for BSA + *p*-MAC-Calix system). Apparently, the $K_{LB}$ are relatively large. Whereas the corresponding dissociation constant $K_D$ ($K_D = 1.2538 \times 10^{-5}$ mol/L for BSA + *o*-MAC-Calix system, $K_D = 1.7270 \times 10^{-5}$ mol/L for BSA + *m*-MAC-Calix system and $K_D = 2.1598 \times 10^{-5}$ mol/L for BSA + *p*-MAC-Calix system) were quite small. This result estimates that the quenching is static process [36]. In addition, from Table 1, it could be found that all of these Lineweaver–Burk plots had better linear relationship ($R^2$ = 0.9994 for BSA + *o*-MAC-Calix system, $R^2$ = 0.9997 for BSA + *m*-MAC-Calix system and $R^2$ = 0.9976 for BSA + *p*-MAC-Calix system) than the corresponding Stern–Volmer plots. Thus, it can be confirmed again that the fluorescence quenching mechanism of azocalix[4]arene derivatives to BSA is mainly static quenching procedure indeed.

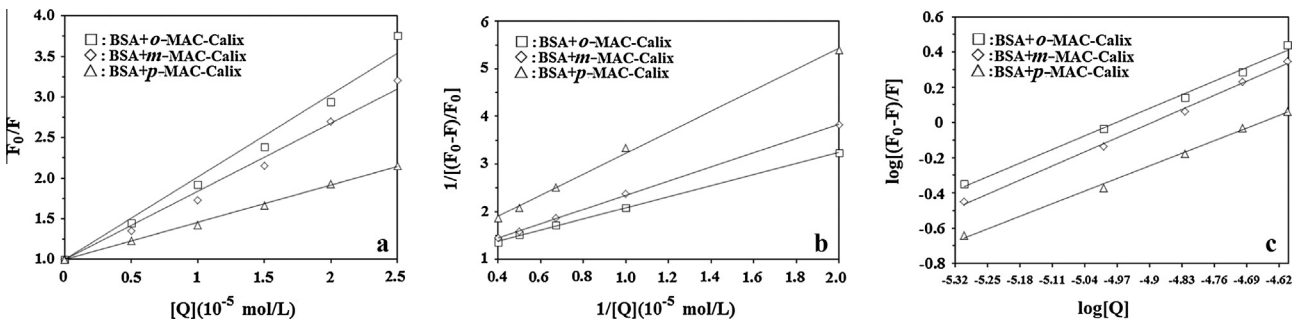


**Fig. 2.** Stern–Volmer plot (a), Lineweaver–Burk plot (b) and double logarithm plot (c) of BSA + *o*-MAC-Calix, BSA + *m*-MAC-Calix and BSA + *p*-MAC-Calix solutions with *o*-MAC-Calix, *m*-MAC-Calix and *p*-MAC-Calix concentrations (from $0.00 \times 10^{-5}$ mol/L to $2.50 \times 10^{-5}$ mol/L at $0.50 \times 10^{-5}$ mol/L intervals) ([BSA] = $1.00 \times 10^{-5}$ mol/L, [Tris–HCl] = [NaCl] = 50 mmol/L, pH = 7.40, $T_{solu}$ = 37.00 ± 0.02 °C and $V_{total}$ = 25.00 mL).

According to Fig. 2c, the equilibrium constants ($K_A$) and the binding site numbers ($n$) could be calculated by using the double logarithm Eq. (3).

$$\log[(F_0 - F)/F)] = \log K_A + n \log[Q_F] \quad (3)$$

The results were shown in Table 1, $K_A$ and $n$ could be measured from the intercept and slope by plotting $\log[(F_0 - F)/F)]$ against $\log[Q_F]$. Obviously, being similar to the $K_{LB}$, the array order was also $K_{A(BSA+o\text{-MAC-Calix})} > K_{A(BSA+m\text{-MAC-Calix})} > K_{A(BSA+p\text{-MAC-Calix})}$. It illustrates that *o*-MAC-Calix has more efficient binding to BSA molecules than *m*-MAC-Calix and *p*-MAC-Calix. The reason may be that the bonding site of the methyl on azocalix[4]arene derivatives affect the interaction with BSA. The methyl of azo group are in the ortho-position so that the *o*-MAC-Calix gets hydrophobic interaction with BSA easier. The three $n$ values are equal to about 1, indicating that there is the same type of binding site for azocalix[4]arene derivatives to BSA.

Furthermore, the titration curve of BSA with the addition of azocalix[4]arene derivatives were used to prove the binding site number ($n$). The initial fluorescence intensity of BSA started to decrease as a function of increasing concentration of azocalix[4]arne and reached an approximately saturation point after the addition of 1 equiv azocalix[4]arene derivatives (Fig. 3). It indicates the binding site number ($n$) is in line with the data calculated according to the double logarithm equation, which strongly suggests the existence of a single binding site in BSA protein.

Utilizing $K_A$, the free energy change ($\Delta G^0$) could be calculated from the relationship (4):

$$\Delta G^0 = -RT \ln K_A \quad (4)$$

Here, $R = 8.314$ J/mol·K and $T = 310$ K, and the $\Delta G^0$ were −32.604 kJ/mol for BSA + *o*-MAC-Calix system, −33.149 kJ/mol for BSA + *m*-MAC-Calix system and −28.177 kJ/mol for BSA + *p*-MAC-Calix system. The negative sign for $\Delta G^0$ indicates that the binding of azocalix[4]arene derivatives to BSA molecule is spontaneous.

### 3.3. Binding distances between BSA with azocalix[4]arene derivatives (*o*-MAC-Calix, *m*-MAC-Calix and *p*-MAC-Calix)

In the preceding paragraph, the interactions of three azocalix[4]arene derivatives with BSA molecules could be speculated through the fluorescence quenching of BSA solutions along with the increase of azocalix[4]arene derivatives concentration. The binding distance ($r$) between BSA and azocalix[4]arene derivatives could be determined according to Foster's non-radioactive energy transfer theory (FRET) [37,38]. Based on this theory, the efficiency ($E$) of energy transfer between the donor (BSA) and acceptor could be calculated by using Eq. (5):

$$E = 1/\left[1 + (r/R_0)^6\right] \quad (5)$$

where $r$ is the binding distance between the donor and acceptor, and $R_0$ is the critical binding distance when the efficiency ($E$) of energy transfer is 50%, which could be calculated by the Eq. (6):

$$R_0^6 = 8.8 \times 10^{-25}(K^2 n^{-4} \varphi_D J) \quad (6)$$

where the $K^2$ is the spatial orientation factor of the dipole, $n$ is the refractive index of medium, $\varphi_D$ is the quantum yield of the donor in the absence of acceptor and $J$ is the overlap integral of the emission spectrum of the donor and the absorption spectrum of the acceptor. In the present case, $K^2$, $n$ and $\varphi_D$ are 2/3, 1.336 and 0.15 for BSA, respectively. And then, the $J$ could be calculated by the Eq. (7).

$$J = \sum F(\lambda)\varepsilon(\lambda)\lambda^4 \Delta\lambda / \sum F(\lambda)\Delta\lambda \quad (7)$$

where the $\lambda$ is the wavelength of fluorescence spectrum of BSA and maximum absorption wavelength of azocalix[4]arene derivative. The $F(\lambda)$ is the fluorescence intensity of BSA and the $\varepsilon$ ($\lambda$) is the absorbance of azocalix[4]arene derivative at $\lambda$. Fig. 4 showed the spectral overlap of fluorescence emission of BSA solution and UV–vis absorption of azocalix[4]arene derivatives solutions at 200–500 nm, respectively. The efficiency ($E$) of energy transfer could be determined by the Eq. (8):

$$E = 1 - F/F_0 \quad (8)$$

where $F_0$ and $F$ are the fluorescence intensities of BSA solutions with $1.0 \times 10^{-5}$ mol/L at 345 nm in the absence and presence of azocalix[4]arene derivatives with $1.0 \times 10^{-5}$ mol/L, respectively. According to the above equations from (4)–(8), $E$, $R_0$ and $J$ could be calculated and the corresponding results were given in Table 2.

The binding distances ($r$) between BSA and azocalix[4]arene derivatives were calculated and the corresponding results were 2.2902 nm for BSA + *o*-MAC-Calix system, 2.6508 nm for BSA + *m*-MAC-Calix system and 2.7194 nm for BSA + *p*-MAC-Calix system. The connection of azocalix[4]arene derivatives with BSA may be formed due to the hydrogen bond, benzene ring stacking, the hydrophobic interaction of the methyl was showed in Fig. 5. The benzene ring stacking and hydrogen bond are almost same between azocalix[4]arene and BSA molecular. However, their hydrophobic interactions display some differences, because hydrophobic interactions depend on the distance and angle between methyl group of azobenzene and BSA molecules. The *o*-MAC-Calix may be easier forming hydrophobic interaction with BSA than the other two azocalix[4]arene derivatives. Therefore, the order of binding intensity is *o*-MAC-Calix-BSA > *m*-MAC-Calix-BSA > *p*-MAC-Calix-BSA. This result is consistent with the $K_A$ previously obtained. Apparently, the binding distances of three azocalix[4]arene derivatives with BSA are all less than 7.0 nm, which indicates that the energy transfer from BSA to azocalix[4]arene derivatives occur with high possibility [39]. It also suggests that the fluorescence quenching of BSA molecule is through energy transfer from BSA to corresponding azocalix[4]arene.

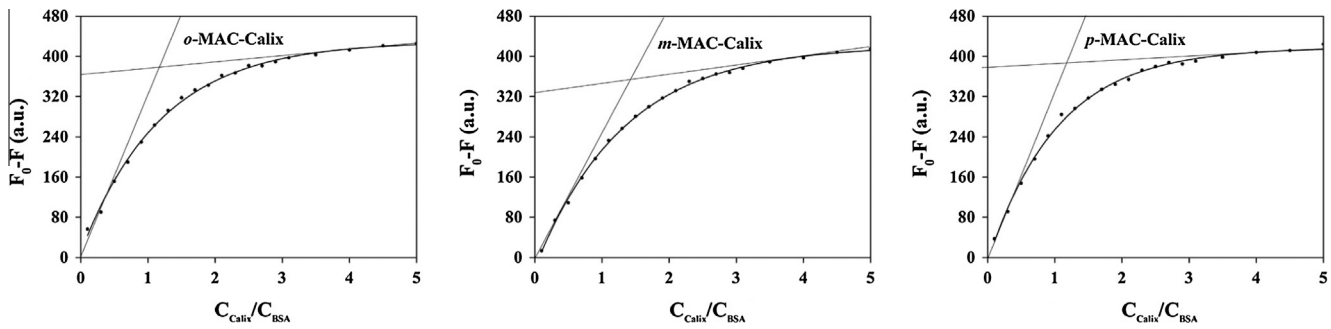


**Fig. 3.** The titration curve of BSA with the addition of azocalix[4]arene derivatives(o-MAC-Calix, m-MAC-Calix and p-MAC-Calix) ([BSA] = $1.00 \times 10^{-5}$ mol/L, [Tris–HCl] = [NaCl] = 50 mmol/L, pH = 7.40, $T_{solu}$ = 37.00 ± 0.02 °C and $V_{total}$ = 25.00 mL).

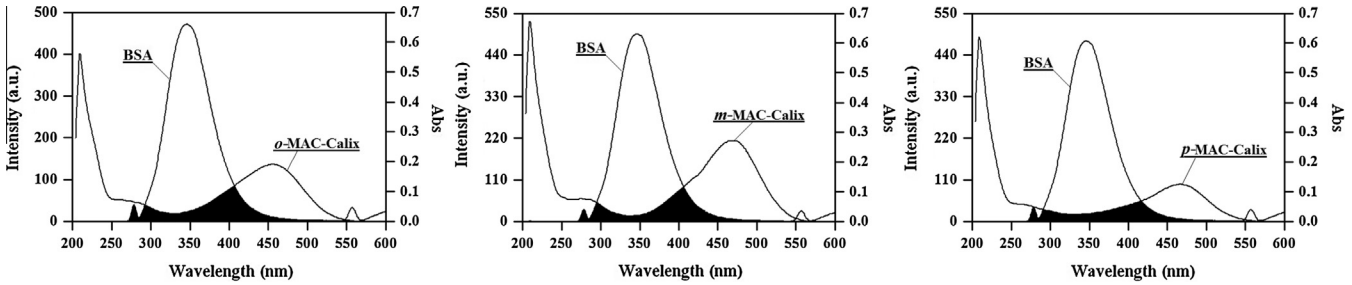


**Fig. 4.** Spectral overlap of fluorescence ($\lambda_{ex}$ = 278 nm) of BSA solution and absorption of BSA + *o*-MAC-Calix, BSA + *m*-MAC-Calix and BSA + *p*-MAC-Calix solutions ([BSA] = [*o*-MAC-Calix] = [*m*-MAC-Calix] = [*p*-MAC-Calix] = 1.00 × $10^{-5}$ mol/L, [Tris–HCl] = [NaCl] = 50 mmol/L, pH = 7.40, $T_{solu}$ = 37.00 ± 0.02 °C and $V_{total}$ = 25.00 mL).

**Table 2**
Energy transfer efficiency (*E*), critical binding distance (*R*), overlap integral (*J*) and binding distance (*r*) calculated according to Foster's non-radioactive energy transfer theory ([BSA] = [*o*-MAC-Calix] = [*m*-MAC-Calix] = [*p*-MAC-Calix] = 1.00 × $10^{-5}$ mol/L, [Tris–HCl] = [NaCl] = 50 mmol/L, pH = 7.40, $T_{solu}$ = 37.00 ± 0.02 °C and $V_{total}$ = 25.00 mL).

| System | *E* (%) | *R* (nm) | *J* ($cm^3$·L/mol) | *r* (nm) |
|---|---|---|---|---|
| *o*-MAC-Calix | 48.01 | 2.5560 | 1.00949 × $10^{-14}$ | 2.2902 |
| *m*-MAC-Calix | 42.15 | 2.5147 | 9.15440 × $10^{-15}$ | 2.6508 |
| *p*-MAC-Calix | 29.90 | 2.3594 | 6.24610 × $10^{-15}$ | 2.7194 |

### *3.4. Synchronous fluorescence spectra of BSA + o-MAC-Calix, BSA + m-MAC-Calix and BSA + p-MAC-Calix solutions*

Synchronous fluorescence spectroscopy technique was introduced by Lloyd [40]. Its spectra could provide much valuable information about the microenvironment around fluorogens in biomolecules [41]. For protein molecules, when the $\Delta\lambda$ = 15 nm is fixed, the spectrum characteristic of Tyr residues can be observed, and when $\Delta\lambda$ = 60 nm is done, the spectrum characteristic of Trp residues can be obtained in general [42,43]. In this research, the

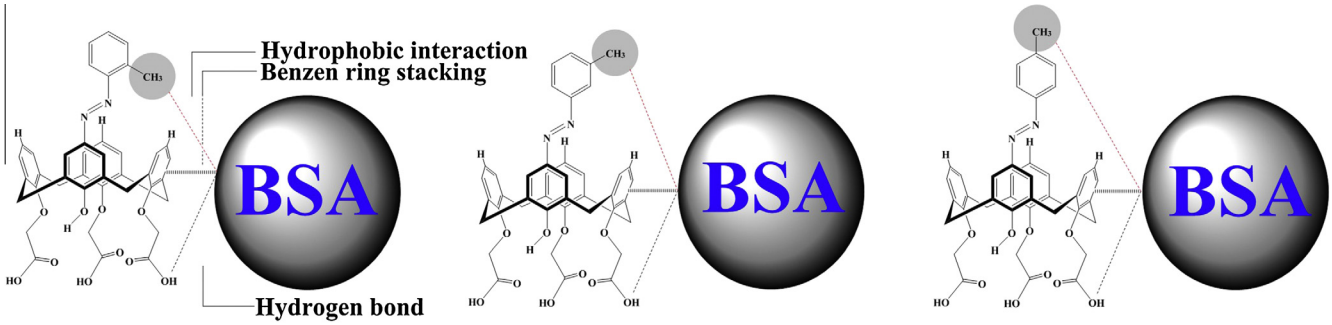


**Fig. 5.** Difference of hydrophobic interaction of BSA + azocalix[4]arene derivatives (*o*-MAC-Calix, *m*-MAC-Calix or *p*-MAC-Calix).

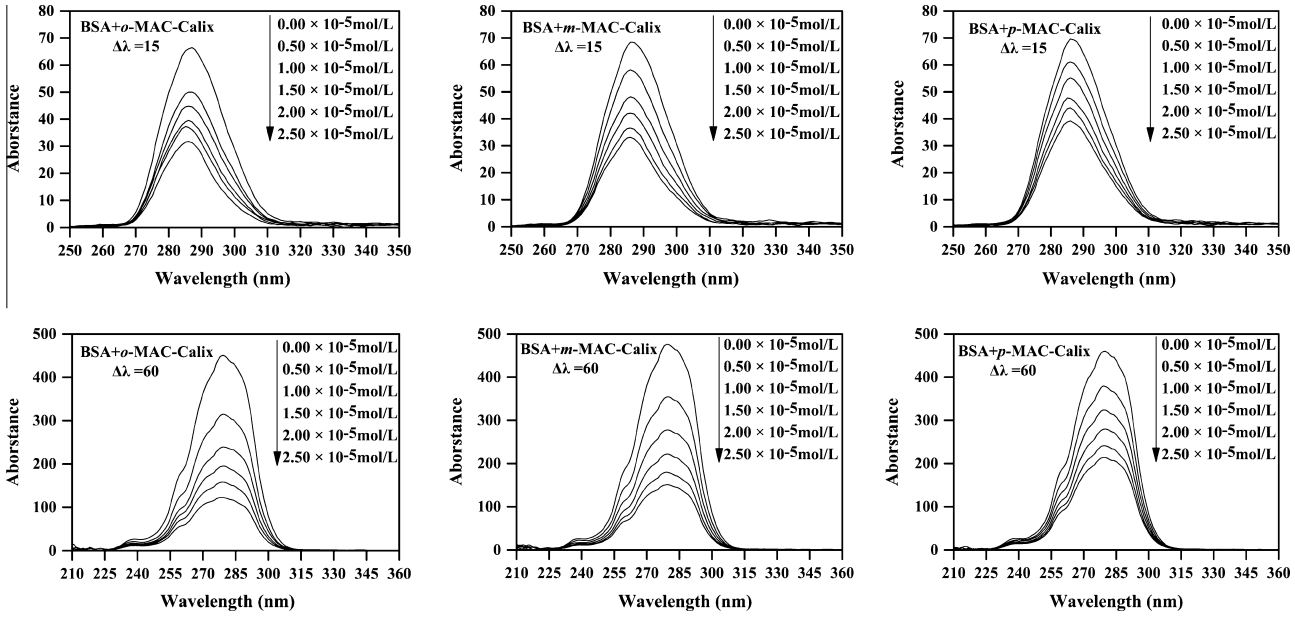


**Fig. 6.** Synchronous fluorescence spectra of BSA + *o*-MAC-Calix, BSA + *m*-MAC-Calix and BSA + *p*-MAC-Calix solutions with *o*-MAC-Calix, *m*-MAC-Calix and *p*-MAC-Calix concentrations (from 0.00 × $10^{-5}$ mol/L (o) to 2.50 × $10^{-5}$ mol/L (e) at 0.50 × $10^{-5}$ mol/L intervals) ([BSA] = 1.00 × $10^{-5}$ mol/L, [Tris–HCl] = [NaCl] = 50 mmol/L, pH = 7.40, $T_{solu}$ = 37.00 ± 0.02 °C and $V_{total}$ = 25.00 mL).

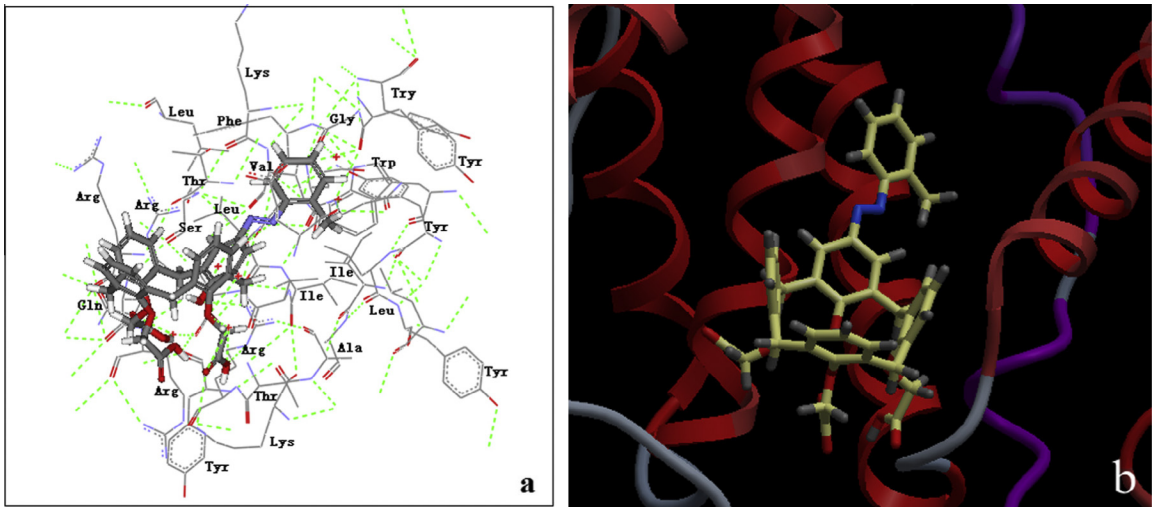


**Fig. 7.** (a) Docking model of *o*-MAC-Calix at the active sites of BSA. (b) Minimum energy docking conformation obtained from docking simulation. The BSA is presented by ribbon structure whereas *o*-MAC-Calix by stick model.

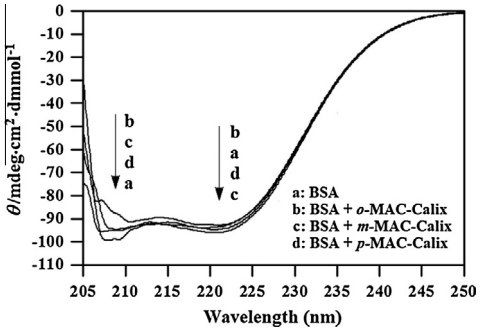


**Fig. 8.** CD spectras of BSA + azocalix[4]arene derivatives (*o*-MAC-Calix, *m*-MAC-Calix or *p*-MAC-Calix) solutions. ([BSA] = [*o*-MAC-Calix] = [*m*-MAC-Calix] = [*p*-MAC-Calix] = $1.0 \times 10^{-5}$ mol $L^{-1}$, pH = 7.40, [NaCl] = 50 mmol $L^{-1}$, $T_{solu}$ = 37.0 ± 0.2 °C and $V_{total}$ = 25.00 mL).

synchronous fluorescence spectroscopy was used to estimate the binding site of azocalix[4]arene derivatives to BSA molecules.

From Fig. 6, it could be seen that three courses the fluorescence intensities at $\Delta\lambda$ = 15 nm (upper) and $\Delta\lambda$ = 60 nm (nether) both decreased gradually with the increase of azocalix[4]arene derivatives. Three azocalix[4]arene derivatives have stronger fluorescence intensity for $\Delta\lambda$ = 60 nm than for $\Delta\lambda$ = 15 nm. It proves that three azocalix[4]arene derivatives can bind the Trp residues much stronger than Tyr residues.

In order to illustrate the *o*-MAC-Calix has better hydrophobic interaction. Molecular docking experiment was been used. Based on the Molegro Virtual Docker docking, the *o*-MAC-Calix is located at the active sites, which is on the surface of the BSA. It could be seen that the Trp residue of BSA molecular had strong interaction with *o*-MAC-Calix, as seen in Fig. 7a. This result is consistent with the experimental data above-mentioned. From Fig. 7b, the minimum energy docking conformation was obtained in docking simulation. It shows that the *o*-MAC-Calix is embedded in the hydrophobic cavity of helical structure of BSA molecular, which may be due to the strong hydrophobic interaction between methyl group of azobenzene and BSA molecule.

### *3.5. Circular dichroism (CD) spectra of BSA, BSA + o-MAC-Calix, BSA + m-MAC-Calix and BSA+p-MAC-Calix solutions*

CD spectroscopy is one of the most powerful techniques for examining the conformational changes of proteins whose bound state may affect their secondary structure [44]. As we know, the CD spectra of BSA exhibits two negative bands at 208 and 222 nm, which are characteristics of α-helix structure of proteins. The band at 208 nm corresponds to $\pi \rightarrow \pi^*$ transition of the α-helix, whereas the band at 222 nm corresponds to $n \rightarrow \pi^*$ transition of the α-helix [45,46]. In general situation, the α-helix content of BSA could decrease along with the increase of micromolecule compound concentration. From Fig. 8, it could be seen that the negative peak decreases (curves *b*, *c* and *d*) comparing with that of BSA original solution (curve *a*) at 208 nm when the BSA molecules were mixed with azocalix[4]arene derivatives in Tris–HCl–NaCl buffer solution. It is proves that the helicity of BSA decreased significantly with adding azocalix[4]arene derivatives [45,47]. And the decreasing degree is *o*-MAC-Calix > *m*-MAC-Calix > *p*-MAC-Calix. However, the negative peaks of BSA (curves *b*, *c* and *d*) slightly increase when *m*-MAC-Calix and *p*-MAC-Calix added to BSA at 222 nm. It may be due to the presence of potential chirality of *m*-MAC-Calix and *p*-MAC-Calix, which maintains or increases α-helix content of BSA molecules [48].

## 4. Conclusion

In this paper, three water-soluble azocalix[4]arene derivatives (*o*-MAC-Calix, *m*-MAC-Calix and *p*-MAC-Calix) were synthesized. Their interactions with BSA molecules in Tris–HCl–NaCl buffer solution were studied by fluorescence spectroscopy. The experimental results shows that three azocalix[4]arene derivatives could all bind to BSA molecules obviously, and then quenched their intrinsic fluorescence efficiently. According to the fluorescence quenching calculation, the bimolecular quenching constant ($K_q$), apparent quenching constant ($K_{sv}$), equilibrium constants ($K_A$), corresponding dissociation constant ($K_D$) and binding site number ($n$) were measured. The quenching mechanisms are all static process. In addition, the synchronous fluorescence spectroscopy indicates that three azocalix[4]arene derivatives were more vicinal to Trp residues than Tyr residues. The CD spectroscopy shows the content of α-helix changing under the effect of azocalix[4]arene derivatives. It is expected that this work could offer some valuable references for promoting the application of calixarene derivatives in the biological field.

## Acknowledgments

The authors greatly acknowledge the National Natural Science Foundation of China (No. 21171081), the Science Foundation of

the Education Department of Liaoning Province (No. L2011007) and the Science and Technology Planning Project of Shenyang Technology Bureau (No. F13-318-1-51) for financial supports. The authors thank Molegro ApS for kindly providing a free evaluation copy of their software package and the laboratory of Prof. Chun Hu of Shenyang Pharmaceutical University. The authors also would like to thank our colleagues and other students for their participating in this work.

## Appendix A. Supplementary material

Supplementary data associated with this article can be found, in the online version, at http://dx.doi.org/10.1016/j.bioorg.2014.12.002.

## References

[1] M. Dey, C.P. Rao, P. Saarenketo, K. Rissanen, E. Kolehmainen, Eur. J. Inorg. Chem. (2002) 2207–2215.
[2] R.K. Pathak, S.M. Ibrahim, C.P. Rao, Tetrahedron Lett. 50 (2009) 2730–2734.
[3] R.K. Pathak, A.G. Dikundwar, T.N. Guru Row, C.P. Rao, Chem. Commun. 46 (2010) 4345–4347.
[4] A. Mitra, A.K. Mittal, C.P. Rao, Chem. Commun. 47 (2011) 2565–2567.
[5] R. Joseph, J.P. Chinta, C.P. Rao, Inorg. Chem. 50 (2011) 7050–7058.
[6] H.M. Chawla, R. Srivastava, S.N. Sahu, S. Kumar, S. Upreti, Supramol. Chem. 24 (2012) 672–683.
[7] S. Patra, R. Gunupuru, R. Lo, E. Suresh, B. Ganguly, P. Paul, New J. Chem. 36 (2012) 988–1002.
[8] N.J. Wang, C.M. Sun, W.S. Chung, Sens. Actuators B 171–172 (2012) 984–993.
[9] R.K. Pathak, V.K. Hinge, P. Mondal, C.P. Rao, Dalton Trans. 41 (2012) 10652–10660.
[10] M. Tabakci, B. Tabakci, A.D. Beduk, Tetrahedron 68 (2012) 4182–4186.
[11] J.Y. Zhan, X.L. Zhu, F. Fang, F.J. Miao, D.M. Tian, H.B. Li, Tetrahedron 68 (2012) 5579–5582.
[12] V.V.S. Mummidivarapu, V.K. Hinge, K. Tabbasum, R.G. Gonnade, C.P. Rao, J. Org. Chem. 78 (2013) 3570–3576.
[13] V.V.S. Mummidivarapu, K. Tabbasum, J.P. Chinta, C.P. Rao, Dalton Trans. 41 (2012) 1671–1674.
[14] Y. Xue, Y. Guan, A.N. Zheng, H.N. Xiao, Colloids Surf. B: Biointerfaces 101 (2013) 55–60.
[15] L.K. Tsou, G.E. Dutschman, E.A. Gullen, M. Telpoukhovskaia, Y.C. Cheng, A.D. Hamilton, Bioorg. Med. Chem. Lett. 20 (2010) 2137–2139.
[16] M. Mourer, N. Psychogios, G. Laumond, A.M. Aubertin, J.B. Regnouf-de-Vains, Bioorg. Med. Chem. Lett. 18 (2010) 36–45.
[17] M. Mourer, R.E. Duval, C. Finance, J.B. Regnouf-de-Vains, Bioorg. Med. Chem. Lett. 16 (2006) 2960–2963.
[18] C. Geller, S. Fontanay, M. Mourer, H.M. Dibama, J.B. Regnouf-de-Vains, C. Finance, R.E. Duval, Antiviral Res. 88 (2010) 343–346.
[19] G.M.L. Consoli, G. Granata, E. Galante, I.D. Silvestro, L. Salafia, C. Geraci, Tetrahedron 63 (2007) 10758–10763.
[20] W. Janrungroatsakul, T. Vilaivan, C. Vilaivan, S. Watchasit, C. Suksai, W. Ngeontae, W. Aeungmaitrepirom, T. Tuntulani, Talanta 105 (2013) 1–7.
[21] J.B. Chao, H.F. Wang, Y.B. Zhang, F.J. Huo, C.X. Yin, Spectrochim. Acta Part A Mol. Biomol. Spectrosc. 103 (2013) 73–78.
[22] M. Dudic, A. Colombo, F. Sansone, A. Casnati, G. Donofrio, R. Ungaro, Tetrahedron 60 (2004) 11613–11618.
[23] F. Sansone, M. Dudic, G. Donofrio, C. Rivetti, L. Baldini, A. Casnati, S. Cellai, R. Ungaro, J. Am. Chem. Soc. 128 (2006) 14528–14536.
[24] V. Bagnacani, F. Sansone, G. Donofrio, L. Baldini, A. Casnati, R. Ungaro, Org. Lett. 10 (2008) 3953–3956.
[25] J.E. Patterson, D.M. Geller, Biochem. Biophys. Res. Commun. 74 (1977) 1220–1226.
[26] R.T.A. McGillivray, D.W. Chung, E.W. Davie, Eur. J. Biochem. 98 (1979) 477–485.
[27] K. Hirayama, S. Akashi, M. Furuya, K.I. Fukuhara, Biochem. Biophys. Res. Commun. 173 (1990) 639–646.
[28] X.M. He, D.C. Carter, Nature 358 (1992) 209–215.
[29] X.L. Han, F.F. Tian, Y.S. Ge, F.L. Jiang, L. Lai, D.W. Li, Q.L.Y. Yu, J. Wang, J. Photochem. Photobiol. B: Biol. 109 (2012) 1–11.
[30] M. Lee, W.G. An, J.H. Kim, H.J. Choi, S.H. Kim, M.H. Han, K. Koh, Mater. Sci. Eng., C 24 (2004) 123–126.
[31] J. Gualbert, P. Shahgaldian, A.W. Coleman, Int. J. Pharm. 257 (2003) 69–73.
[32] C.D. Gutsche, B. Dhawan, K.H. No, R. Muthukrishnan, J. Am. Chem. Soc. 103 (1981) 3782–3792.
[33] I. Aoki, T. Harada, T. Sakaki, Y. Kawahara, S. Shinkai, J. Chem. Soc., Chem. Commun. 730 (1992) 1341–1345.
[34] K.C. Chang, I.H. Su, G.H. Lee, W.S. Chung, Tetrahedron Lett. 48 (2007) 7274–7278.
[35] T. Yoneyama, H. sadamatsu, S. Kuwata, H. Kawakita, K. Ohto, Talanta 88 (2012) 121–128.
[36] J.Q. Gao, Y.W. Guo, J. Wang, Z.Q. Wang, X.D. Jin, C.P. Cheng, Y. Li, K. Li, Spectrochim. Acta Part A: Mol. Biomol. Spectrosc. 78 (2011) 1278–1286.
[37] Y.J. Hu, Y. Liu, R.M. Zhao, J.X. Dong, S.S. Qu, J. Photochem. Photobiol. A: Chem. 179 (2006) 324–329.
[38] J. Kang, Y. Liu, M.X. Xie, S. Li, M. Jiang, Y.D. Wang, Biochim. Biophys. Acta (BBA) – Gen. Subjects 1674 (2004) 205–214.
[39] M. Guo, W.J. Lu, M.H. Li, W. Wang, Eur. J. Med. Chem. 43 (2008) 2140–2144.
[40] J.B.F. Lloyd, Nat. Phys. Sci. 231 (1971) 64–65.
[41] T. Yuan, A.M. Weljie, H.J. Vogel, Biochemistry 37 (1998) 3187–3195.
[42] J.N. Miller, Proc. Anal. Div. Chem. Soc. 16 (1979) 203–208.
[43] B. Klajnert, M. Bryszewska, Bioelectrochemistry 55 (2002) 33–35.
[44] A. Nozaki, M. Hori, T. Kimura, H. Ito, T. Hatano, Chem. Pharm. Bull. 57 (2009) 224–228.
[45] Q.S. Wang, P.F. Liu, X.L. Zhou, X.L. Zhang, T.T. Fang, P. Liu, X.M. Min, X. Li, J. Photochem. Photobiol. A: Chem. 230 (2012) 23–30.
[46] V.M. Bolaños-García, S. Ramos, R. Castillo, J. Xicohtencatl-Cortes, J. Mas-Oliva, J. Phys. Chem. B 105 (2001) 5757–5765.
[47] H.K. Mandal, A. Kundu, S. Balti, A. Mahapatra, J. Colloid Interface Sci. 378 (2012) 110–117.
[48] M.M. Zou, Y. Li, J. Wang, Q. Wang, J.Q. Gao, Q. Yang, P. Fan, Ultrason. Sonochem. 20 (2013) 685–695.